

TESTS OF RICH PHOTON DETECTORS FOR THE HERA-B EXPERIMENT

P. Križan^{1,2}, S. Korpar⁴, M. Starič¹, A. Stanovnik^{1,3}, M. Cindro¹, D. Škrk¹, M. Zavrtanik¹, W. Schmidt-Parzefall⁵, T. Hamacher⁶, E. Michel⁶ and P. Weyers⁶

- (¹) *J. Stefan Institute, University of Ljubljana, Ljubljana, Slovenia*,
 (²) *Faculty of Natural Sciences and Technology, University of Ljubljana, Ljubljana, Slovenia*
 (³) *Faculty of Electrical Engineering and Computer Sciences, University of Ljubljana, Ljubljana, Slovenia*
 (⁴) *Technical Faculty, University of Maribor, Maribor, Slovenia*
 (⁵) *II. Institut für Experimentalphysik, Universität Hamburg, Germany*
 (⁶) *DESY, Hamburg, Germany*

A multiwire proportional chamber with CsI photocathode pads and a TMAE based photon detector have been tested in order to evaluate their potential as candidates for a fast ring imaging Cherenkov counter, to be used for separation of pions from kaons in the HERA-B experiment proposed at DESY. Results of the tests are presented and the following parameters are discussed: the number of photons detected per ring, resolution of the Cherenkov angle, photoelectron drift time distribution, fraction of clusters and avalanche photon feedback.

1. Introduction

The HERA-B experiment proposed at DESY intends to study CP violation in the B meson system [1]. The spectrometer includes a Ring Imaging Cherenkov (RICH) detector, which should be capable of a 3σ separation of kaons from pions up to 90 GeV/c. In addition to a good resolution of Cherenkov angle, the detector should resolve hits belonging to successive beam crossings, which occur every 96 ns. Each beam bunch is estimated to give rise to 5 events with about 200 tracks of which approximately half radiate Cherenkov photons. The detector should thus be capable of withstanding high rates (~ 100 kHz per 8×8 mm² pad) for prolonged periods (\sim months) with little reduction in performance.

The tests described in the present work aim at obtaining direct experimental results on some of the parameters and at comparing two different types of detectors envisaged for Cherenkov ring imaging. The photosensitive component in the first detector is TMAE vapour, which is added to the chamber gas. The second detector uses a reflective solid CsI photocathode, which has been shown to have a quantum efficiency comparable to that of TMAE [2].

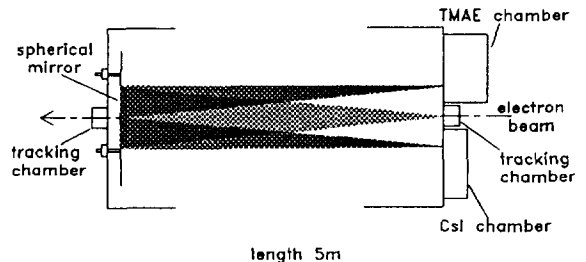


Figure 1. Experimental lay-out for tests of the two photon detectors.

2. Experimental set-up

The detectors were tested with Cherenkov radiation of 3 GeV/c electrons in a 5 m long NTP argon gas radiator (Fig.1). The T24 test beam at DESY in Hamburg, enters and exits the gas tank ($\ell = 5$ m, $\Phi = 80$ cm) through multiwire chambers, which measure the direction of each incident electron. A spherical mirror on the inside of the beam exit flange, reflects the Cherenkov photons to the focal plane at the beam entrance flange, where each of the two photon detectors measures part of the Cherenkov ring. A scintilla-

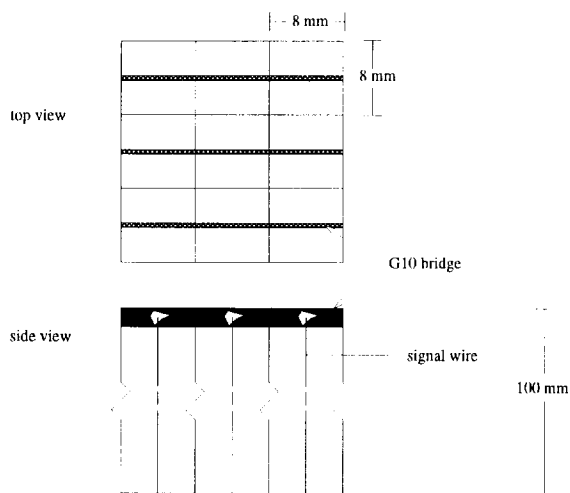


Figure 2. The geometry of the TMAE detector.

tion counter in front of the beam entrance MWPC was used for timing.

The TMAE detector is composed of cells with cross section $8 \times 8 \text{ mm}^2$ and 100 mm depth in order to reach sufficient absorption of UV photons at room temperature (Fig.2). The walls of the cells are made of gold-coated bronze sheets and a 25 μm diameter anode wire is stretched along the cell axis through the G10 endplate on one side and a G10 bridge on the other [1]. The gas is a TMAE-methane mixture obtained by letting 40% of the methane gas flow through a bubbler at room temperature. The resulting TMAE concentration is somewhat below the optimal value for the maximum of efficient absorption ($\sim 70\%$), which is determined by the initial 5 mm thick dead layer of gas, by the fraction of sensitive chamber surface and by the photon incident angles.

The CsI detector, of dimensions $24 \times 24 \text{ cm}^2$, is an asymmetric multiwire proportional chamber (Fig.3) with $7.5 \times 7.5 \text{ mm}^2$ photocathode pads. The asymmetric geometry allows for higher signals to be obtained from the pads. The chamber gas is pure methane at normal temperature and pressure. Optimized values of the voltages (-560 V on the cathode wires, $+1650 \text{ V}$ on the anode wires and with the photocathode pads at

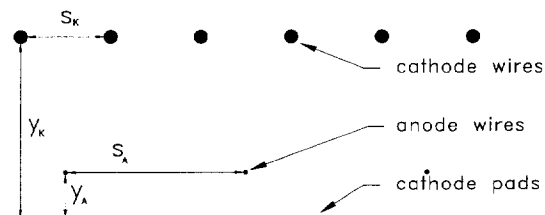


Figure 3. The wire geometry of the CsI detector: $y_k = 2.1 \text{ mm}$, $y_a = 0.66 \text{ mm}$, $s_k = 1.25 \text{ mm}$, $s_a = 2.5 \text{ mm}$

ground potential) allowed a gas gain of about 10^5 without any problems.

The ARGUS μVDC readout system [3] was used for both detectors. The CsI detector used specially designed preamplifiers (conversion gain 8.3 mV/fC, rise time 18 ns, fall time 24 ns, equivalent noise charge 710 electrons and 40 dB common mode RF suppression [4]).

3. Measurements and results

3.1. Number of photoelectrons per ring

The raw data as seen by the two detectors are shown in Fig.4, which represents all the hits accumulated during one run. The average number of detected Cherenkov photons per incident beam electron is 2.0 for the CsI and 3.5 for the TMAE detector. In the case that the entire Cherenkov ring would be intercepted by only one of the detectors, these numbers would normalize to 6.2 photoelectrons/ring for the CsI and 10.2 photoelectrons/ring for the TMAE chamber. Independent tests made with Cherenkov photons emitted by ^{90}Sr β -particles in a 1 cm thick quartz radiator, placed 15 cm downstream of the CsI chamber, showed that the CsI quantum efficiency is only 60 % of the expected value.

Recent measurements of the CsI quantum efficiency [5] gave values in agreement with those obtained by Seguinot et al. [2]. In that work we noted the sensitivity of the CsI quantum efficiency on the substrate material, obtaining better results with Sn/Pb than with copper substrates. We have since then performed additional measurements and found that the CsI quantum efficiency depends also on the polish quality, im-

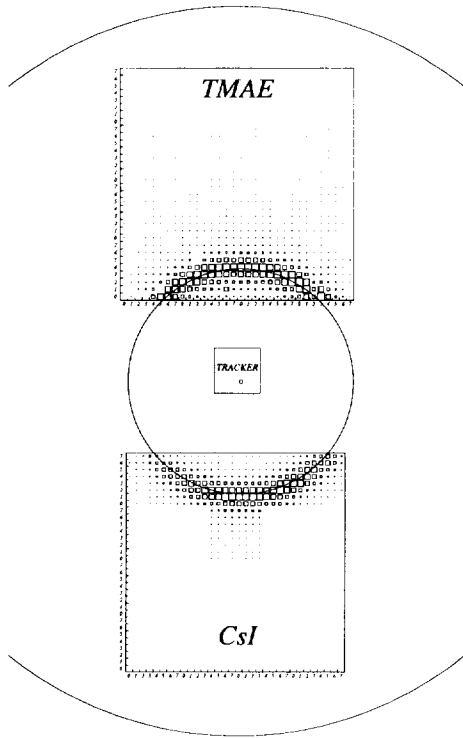


Figure 4. The raw data showing parts of the accumulated Cherenkov rings as seen by the two detectors.

proving when a finer grain polishing paste is used (Fig.5). The photocathode, which is the subject of the present test measurements, has been prepared completely according to the prescription for the highest quantum efficiency. However, a lengthy storage and transportation from Ljubljana to Hamburg presumably resulted in a contamination of the CsI surface and thus in a reduction of the quantum efficiency to 60 % of its normal value.

Assuming the higher value ($RQE = 1$) for the CsI quantum efficiency, the numbers of detected photoelectrons per ring would be equal for both detectors and would amount to about 10 phe/ring. However, calculations based on the density, refractive index and transmission of argon [6], on the reflectivity of the spherical mirror [7], on the absorption in the 5 mm thick quartz windows of both detectors [7], on CsI [5] and

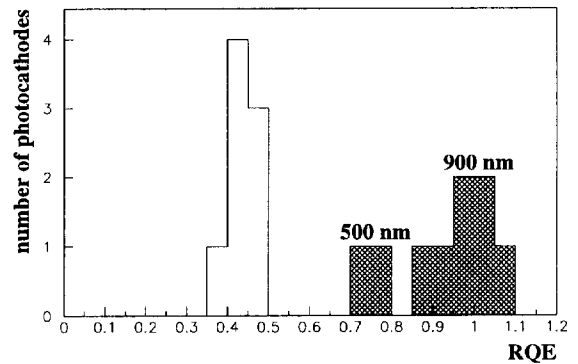


Figure 5. Relative quantum efficiency of CsI photocathodes. RQE is an average ratio of the measured quantum efficiency to that of Seguinot et al. [2]. A $1\mu\text{m}$ diameter grain polishing paste has been used for the higher RQE values (shaded portion of histogram).

TMAE [6] quantum efficiencies, on photoelectron detection efficiencies (90 % for both detectors) and taking into account also the loss of UV photons in the dead layer and walls of the TMAE detector, indicated that each of the two detectors should detect about 20 photoelectrons per ring. The cause of this discrepancy is being investigated, but the most probable reason is that either the mirror reflectivity and/or the radiator gas transmission are lower than expected.

3.2. Resolution of the Cherenkov angle

The granularity of both detectors is about the same ($7.5 \times 7.5 \text{ mm}^2$ pads for CsI and $8 \times 8 \text{ mm}^2$ cells for TMAE) so equal values for the resolution of photon hit positions are expected. The ring radius distribution, calculated from individual hits in the CsI chamber and from the measured direction of the beam electron, is presented in Fig.6. The full width at half maximum (FWHM) of 10 mm corresponds to 0.85 mrad standard deviation of the Cherenkov angle ($\theta_{ch} = 25 \text{ mrad}$) derived from single photon hits. The same value is obtained also for the TMAE detector. Estimates show that the contributions to this number are due mostly to multiple Coulomb scattering of the beam electron in argon ($\sigma_{mcs} \sim 0.64 \text{ mrad}$), to

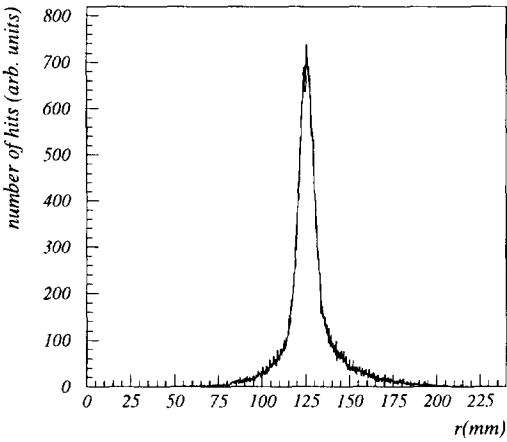


Figure 6. Distribution of the Cherenkov ring radius obtained from single hits in the CsI chamber and from the measured direction of the beam electron.

the pad size ($\sigma_{pad} \sim 0.43$ mrad), to the resolution on the beam particle track direction ($\sigma_{track} \sim 0.2$ mrad) and to mirror imperfections ($\sigma_{mirror} \sim 0.2$ mrad).

By imaging the entire ring with the TMAE chamber alone, the rings shown in Fig.7 have been measured. An iterative procedure to determine the Cherenkov angle without using the electron track information gives the result presented in Fig.8. Multiplying the standard deviation of this distribution ($\sigma=0.17$ mrad) by the square root of the average number of detected photons ($\sqrt{10}$) gives 0.60 mrad. This result is better than the values derived from single photon hits using the charged particle track information. The reason for this discrepancy could be that the Gaussian fit in Fig. 8, does not include the events rejected by the iterative procedure.

3.3. Time spread

The time spread of single photoelectron signals belonging to one Cherenkov ring is essentially due to the spread of the time that the photoelectrons need to drift to the anode wire. The time of each photoelectron pulse was measured relative to the scintillation counter pulse, which corresponds to the entry of a beam electron into the argon gas

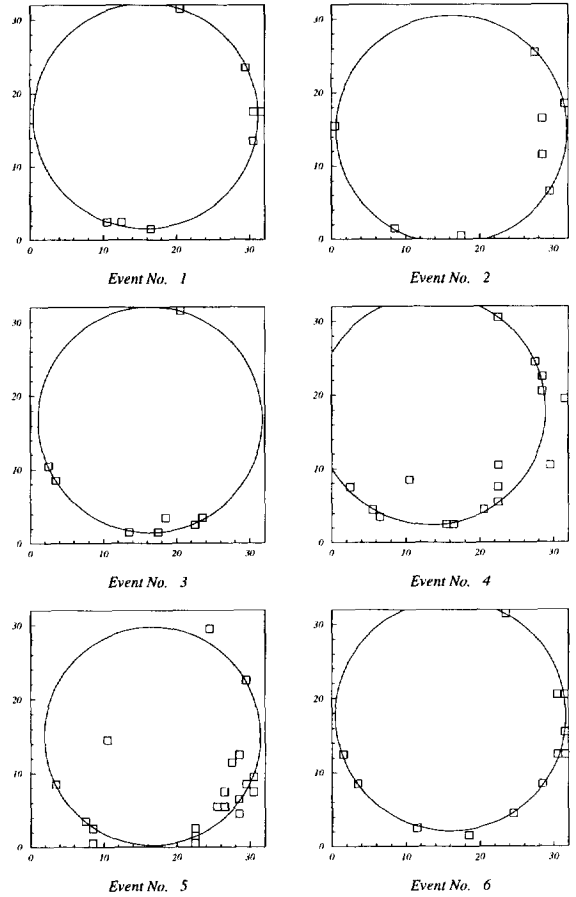


Figure 7. Examples of Cherenkov rings corresponding to single beam electrons as seen by the TMAE detector. The circles are obtained by an iterative method without the use of electron track information.

radiator. The time distributions for both detectors are shown in Fig.9. As expected, the distribution is narrower for the CsI chamber (25 ns time spread) than for the TMAE chamber (65 ns time spread), but for both detectors this spread is smaller than the interval of 96 ns between successive beam bunches in HERA.

A small bump, preceding the main peak is resolved with the CsI detector. This bump is coincident with the beam electron entry into the radiator and is probably due to interactions (bremsstrahlung or knock-on particles) of the

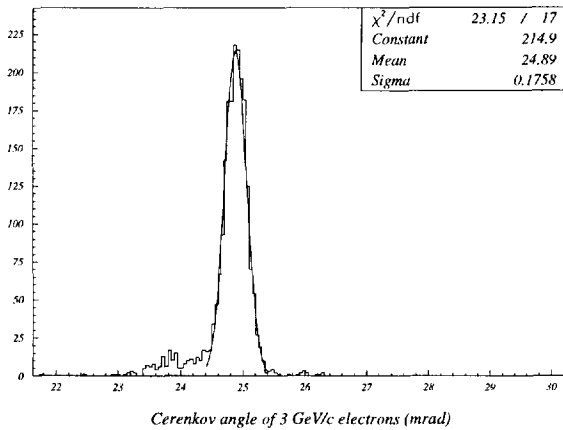


Figure 8. Distribution of Cherenkov angles, obtained with an iterative procedure from photon hits alone, when the entire ring is seen by the TMAE detector.

beam electron upstream of the test apparatus.

3.4. Clusters of hits

One incident photon may fire two or more adjacent pads or cells either as a result of cross-talk and, for the CsI detector, also due to photon feedback or one avalanche inducing pulses on more than one pad. The measured numbers of clusters with at least two adjacent hits (pads or cells) is about 20 % for both detectors (Fig.10). For the TMAE detector, the second hit is more or less evenly distributed around the first (Fig.10). For the CsI detector the axis of both hits is predominantly oriented in the anode wire direction (Fig.10). In this case, the probability of one avalanche inducing pulses on two adjacent pads as well as the possibility of avalanche photon feedback propagation along the wire are both greater than in the direction orthogonal to the wires. Also the common mode RF rejection connects neighbours orthogonal to the anode wire direction, so it might suppress such clusters.

For the CsI detector, the contribution of avalanche photon feedback has been estimated. Monte Carlo calculations of the distribution of photoelectron drift times, which do not take photon feedback into account, reproduce the measured time distribution of only the fastest hit in

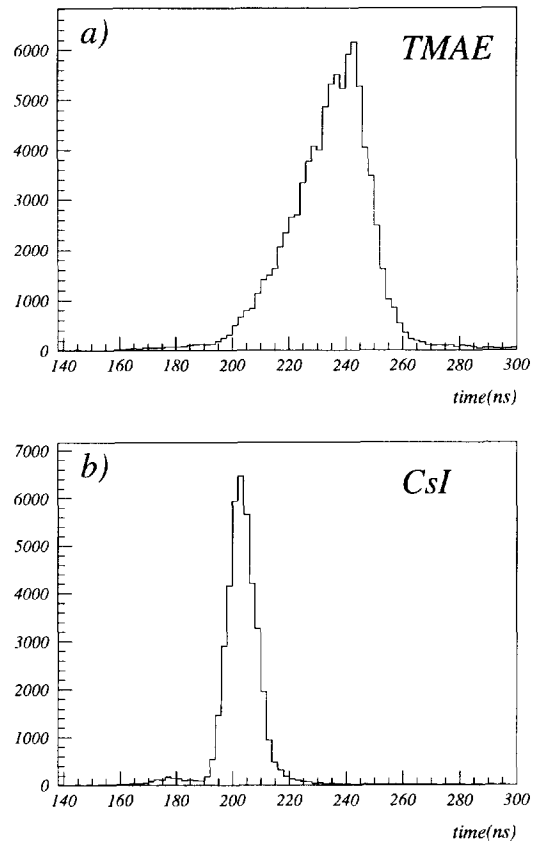


Figure 9. Photoelectron drift time distribution for the TMAE detector and for the CsI detector.

each cluster (Fig.11). The slower pulse in a cluster gives rise to a tail in the distribution, which is not reproduced by such calculations (Fig.11). It is found that for approximately half of all the clusters, the slower signal is delayed for the drift time from the photocathode to the anode wire. The present electrode geometry and applied voltages ($\sim 10^5$ avalanche gain) thus result in about 10 % of avalanche photon feedback.

4. Summary and conclusions

The number of photons detected per Cherenkov ring in the present experiment is lower than expected as a consequence of a decrease in the CsI quantum efficiency (due to storage and transport) and most probably due to a reduced reflectivity

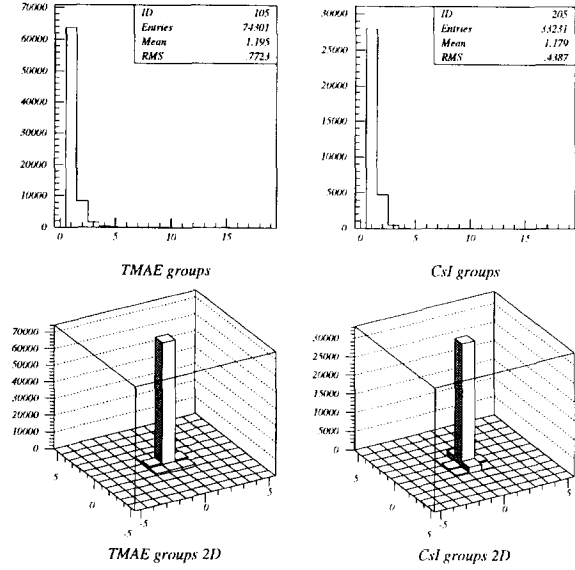


Figure 10. Distributions of clusters depending on the numbers of adjacent hit pads (histograms) and distribution of positions of the slower hit relative to the first hit in the cluster (lego plots).

of the UV mirror or possibly also an increased absorption in the gas radiator.

The rms resolution in the Cherenkov angle, obtained from single photon hits is equal for both detectors and is in agreement with expectations,

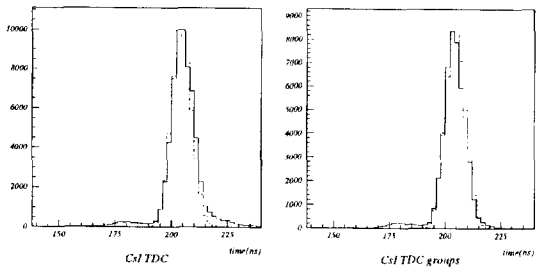


Figure 11. Drift time distribution of only the fastest hit in a cluster (right) and of all the hits (left). Monte Carlo calculations, which do not take photon feedback into account, show an excess of hits, which are delayed relative to the first hit in the cluster.

which predict the largest contributions from multiple Coulomb scattering, pad or cell size, inaccuracy in the measured electron direction and mirror imperfections.

The time spread is narrower for the CsI than for the TMAE detector, but both are good enough for the 96 ns time separation of events belonging to different beam bunches. The fraction of adjacent hit pads (or cells) is about 20 % in both detectors, with half of this being due to avalanche photon feedback in the CsI chamber.

Although the present tests allow some estimates of the parameters for both photon detector types, they do not as yet exclude either possibility. Further measurements will be concentrated on ageing and on detector performance under high rates as are expected in the HERA-B experiment.

Acknowledgements

We are indebted to the OMEGA collaboration for the kind loan of their spherical mirror and we would like to thank the DESY management for the hospitality during our stay in Hamburg, where these tests were performed.

REFERENCES

1. T. Lohse et al., Proposal for HERA-B, DESY-PRC 94/02, May 1994
2. J. Seguinot, G. Charpak, Y. Giomataris, V. Peskov, J. Tischauser, T. Ypsilantis, Nucl. Instr. Meth. in Phys. Res. **297**(1990)133
3. E. Michel et al., Nucl. Instr. Meth. in Phys. Res. **A283** (1989)544
4. M. Zavrtanik, Master thesis, Magistrsko delo, University of Ljubljana, 1994
5. P. Krizan et al., Institute Jožef Stefan report IJS-DP-7087 submitted for publication in Nucl. Instr. Meth. in Phys. Res.
6. J. Seguinot, CERN report EP/89-92
7. R.J. Apsimon et al., Nucl. Instr. Meth. in Phys. Res. **A241**(1985)339